72nd International Astronautical Congress (IAC), Dubai, United Arab Emirates, 25-29 October 2021.

IAC-21-A6.10-B6.5.5

Computationally Efficient Approaches for Low-Thrust Collision Avoidance Activities

Juan Luis Gonzalo[a]*, Camilla Colombo[a], Pierluigi di Lizia[a]

[a] *Department of Aerospace Science and Technology, Politecnico di Milano, Via la Masa 34, Milan, Italy 20156,* juanluis.gonzalo@polimi.it
* Corresponding Author

Abstract

The continuous evolution of low-thrust propulsion technologies, both in performance and the range of platforms that can equip them, provides increasing advantages in propellant efficiency and enables new kinds of missions. However, their smaller control authority compared to impulsive thrusters makes it more challenging to react to unforeseen situations such as collision avoidance activities. Whereas impulsive propulsion allows for efficient Collision Avoidance Manoeuvres (CAMs) performed just a few orbits before the predicted close approach, low thrust CAMs can require a longer acting time. Moreover, low-thrust CAM models are more computationally costly to perform parametric analyses and optimisations to inform the decision-making process.

To tackle some of these issues, we propose analytical and semi-analytical models for low-thrust CAMs, based on averaging techniques and with focus on computational efficiency. They are part of the latest iteration of the Manoeuvre Intelligence for Space Safety (MISS) software tool for CAM design. The main goal in this work is to improve the characterisation of the phasing change at the predicted close approach, as this is the leading contribution to collision probability reduction. To this end, the fully analytical model for constant, tangential low-thrust CAMs introduced in previous works is updated to use a differential time law in eccentric anomaly including first-order terms in thrust acceleration, replacing the previous time law derived from Kepler's equation. Numerical tests show that the new approach significantly improves the accuracy with no additional model complexity, except for quasi-circular orbits. For this case, the zeroth-order time law with a correction for the displacement of the apse line deals better with the singularity of Gauss equations at zero eccentricity. The computational efficiency of the model is leveraged to perform sensitivity analyses for representative test cases, highlight their qualitative characteristics.

Finally, two future improvements and applications are introduced. First, the inclusion of normal thrust acceleration components is treated. Although an analytical result can be obtained, its complexity prevents from using it for efficient CAM computation in its current form. Then, the synergies with machine learning techniques for achieving on-board CAM autonomy are briefly discussed.

Keywords: Collision avoidance manoeuvre, low-thrust, analytical methods, Space Traffic Management, Space Situational Awareness, on-board autonomy

Nomenclature

a	Semi-major axis, km
a_n	Normal thrust acceleration, km/s^2
a_t	Tangential thrust acceleration, km/s^2
b	Semi-minor axis, km
e	Eccentricity
E	Eccentric anomaly, deg or rad
E[·]	Complete elliptic integral of the second kind
f	True anomaly, deg or rad
F[·]	Complete elliptic integral of the first kind
n	Mean motion of the spacecraft, 1/s
r	Orbital radius, km
t	Time, s
v	Orbital velocity (magnitude), km/s
ε	Non-dimensional thrust parameter $a_t/(\mu/a_{ref}^2)$
μ	Gravitational parameter of the primary, km^3/ s^2
ω	Argument of pericentre, deg or rad
Ω	Right ascension of the ascending node, deg or rad

Acronyms/Abbreviations

CA	Close approach
CAM	Collision avoidance manoeuvre
CDM	Conjunction data message
ML	Machine learning
ref	Reference value
RMSE	Root-mean-square error
TCA	Time of closest approach

1. Introduction

Low-thrust propulsion technologies are experiencing a continuous increase both in their performance and the range of platforms that can equip them. Particularly interesting are novel propulsion solutions for small satellites and even CubeSats in Low Earth orbit, enlarging the envelope of missions they can perform. However, although low-thrust propulsion provides significant advantages in propellant efficiency, it also suffers from a smaller control authority compared to impulsive thrusters. This aspect must be considered

during mission design, allocating longer times for phases such as achieving the initial operational orbit or post-mission disposal (when implement). But one of the main challenges is to react to unforeseen situations, including collision avoidance activities. While impulsive propulsion allows for efficient Collision Avoidance Manoeuvres (CAMs) performed just a few orbits before the predicted close approach (CA), low thrust CAMs can require a longer acting time. Moreover, the higher complexity of low thrust CAM models makes it more computationally costly to perform parametrical analyses and optimisations to inform the decision-making process.

Aiming to address this need for efficient computational tools for the design of low-thrust CAMs, this work proposes advanced analytical low-thrust CAM models based on averaging techniques. They expand previous results from the Manoeuvre Intelligence for Space Safety (MISS) software tool [1], which uses Gauss planetary equations to model the orbit modification due to an impulsive or low-thrust-tangential CAM. Two main limitations were identified in the previous models for the low-thrust case [2]. First, to perform the change of independent variable from time to eccentric anomaly, required for the averaging process, an approximate differential time law derived from Kepler's equation was employed. This can have a significant impact on the accuracy of the results, as phasing change at the predicted CA is the leading contribution to collision probability reduction. In [2] a first improvement was proposed by adding the information on the displacement of the line of apses, neglected in the approximate time law, through the variation in argument of pericentre. In this new work, instead, a time law retaining first-order contributions in thrust acceleration is proposed, and its performance is compared with the previous solution for a wide range of values in eccentricity and thrust acceleration. Second, the models in [1][2] are restricted to tangential thrust actions, as they are normally a pseudo-optimal solution for low-thrust CAMs. In the second part of this paper, a first approximation to the development of an analytical formulation of low-thrust CAMs in the normal direction is presented, and future steps are briefly discussed.

One possible application for these analytical CAM models is on-board applications. However, to achieve autonomous operation capabilities, it is also needed to have a decision-making component that, based of space situational information, determines whether the expected risk at the time of the CA exceeds the acceptable threshold and triggers the CAM design. The final part of this paper discusses a framework for autonomous CAM capabilities, proposed as part of the e.Cube CubeSat demonstration mission and using the CAM models in MISS [1].

The rest of this paper is organized as follows. Section 2 presents a brief description of the CAM modelling framework implemented in MISS, highlighting its main blocks and dynamical models. Then, the new time law for the tangential low-thrust case is introduced in Subsection 2.1. Several numerical test cases are presented to characterize the behaviour of the new time law, comparing it with previous approaches. Also, a test case for a representative CA is presented. The discussion on the analytical CAM model is concluded in Subsection 2.2, where the first outcomes for the extension of the model to the normal-thrust case are presented and next steps discussed. Finally, Section 3 briefly introduces the framework for autonomous on-board CAM capabilities, as part of the e.Cube demonstration mission.

2. CAM modelling framework

Let us consider a CA between a manoeuvrable spacecraft and a debris. The spacecraft is equipped with either impulsive of low-thrust propulsion capabilities, and it performs a CAM a given lead time before the predicted time of closest approach (TCA). The effect of this CAM is modelled following the framework presented in [1], composed of three main blocks:

1. Characterization of the orbit modification due to the CAM, expressed in terms of Keplerian elements.
2. Determination of the deviation at the TCA, using linearized relative motion equations to map changes in Keplerian elements at TCA into changes in relative position and velocity [3].
3. Post-processing operations, for analysis and optimization purposes.

These blocks are designed to be highly independent from one another. The mathematical formulation of the first block for impulsive CAMs in an arbitrary direction was already presented in [4][5], together with an analytical expression of the linear state transition matrix of the problem. Instead, the low-thrust case was tackled with increasing level of detail in [6][1][2]. In all cases, Gauss planetary equations are averaged over one revolution to obtain semi-analytical or analytical expressions for the evolution of the Keplerian elements and the change in phasing. To do this, the independent variable has to be changed from time to eccentric anomaly using an approximate time law, as detailed in [1][7]. In all cases, the tangential orientation of thrust was preferred because it is the asymptotically optimal solution for long lead times, and it offers advantages for the analytical manipulations. The first model in [6] was semi-analytical, reducing the evolutions of semi-major axis and eccentricity to their mean secular terms and introducing several corrections for the determination of the change in phasing. However, the neglected oscillatory terms of semi-major axis and eccentricity have an impact on the determination of the phasing change during the last orbital revolution before TCA, which prompted the use of numerical fittings in [1] to approximate these contributions. Both models are semi-

analytical, as they require a numerical integration for the evaluation of the time law during the whole manoeuvre, as well as the numerical integration of the equation for mean anomaly during the last orbital revolution.

To improve both accuracy and computational performance, a recent iteration of the model presented in [2] reached a fully analytical model for semi-major axis, eccentricity, argument of pericentre and time as function of eccentric anomaly. Using this model, the determination of the change in Keplerian elements at the TCA is reduced to a root finding problem in the $t(E)$ time law. Furthermore, the results showed that the solution contains infinite harmonics of eccentric anomaly, explaining the accuracy limitation of the sinusoidal fitting (first harmonic) in [1].

Despite these advances, there are two limitations to be addressed. First, the use of an approximate time law for the change of independent variable prior to averaging sets an upper limit for the attainable accuracy of the model, regardless of the improvements in the analytical or semi-analytical approximate solutions for the resulting system of ODEs. Second, although the approximation of tangential thrust provides good solutions, a more accurate description would require considering also the normal and out-of-plane components. The choice of a more accurate time law is discussed in Subsection 2.1, while the inclusion of the solutions for the normal component is briefly discussed in Subsection 2.2.

2.1 First-order time law

To obtain the single-average of the equations of motion over one revolution, it is first needed to perform a change of independent variable from time to the chosen anomaly, in this case the eccentric anomaly. Both the semi-analytical solution in [6][1] and the analytical one in [2] relied on an approximate differential time law in eccentric anomaly in the form [7][8]:

$$\frac{\mathrm{d}E}{\mathrm{d}t} = \sqrt{\frac{\mu}{a^3}} \frac{1}{1 - e\cos E} \tag{1}$$

where E is the eccentric anomaly, a is the semi-major axis, e is the eccentricity, and μ is the gravitational parameter of the primary. A physical interpretation of this time law can be given considering Kepler's law. Indeed, Eq. (1) can be retrieved by taking the time derivative of Kepler's law, assuming that the derivatives of semi-major axis and eccentricity can be neglected and retaining only the derivative of the eccentric anomaly. This is a reasonable assumption for low-thrust scenarios because the magnitudes of the derivatives of semi-major axis and eccentricity scale with thrust magnitude, whereas eccentric anomaly has to complete a full revolution each period. However, this assumption limits the accuracy of the resulting models. This circumstance was observed and quantified for the analytical model in [2], where the error of the analytical expressions when compared to a high-precision numerical propagation of the equations of motion in eccentric anomaly was smaller than the error between the exact and approximate time laws (both integrated numerically). The importance of the determination of the phasing in a low-thrust deflection was already identified as a key issue in [9], for the case of continuous-thrust deflection of asteroids using single-averaged semi-analytical methods.

A first correction to the approximate time law was proposed in [2], in the form of an apse line correction. In order to capture the small displacements of the line of apses during the manoeuvre, not described by Eq. (1), the change in argument of pericentre was added to the analytical time law resulting from the integration of Eq. (1), using the analytical models for semi-major axis, eccentricity, and argument of pericentre. While this provided significant advantages, a more accurate model can be derived as presented in the following.

In order to retain the effect of thrust in the time law, the full Gauss planetary equations for a constant thrust acceleration a_t are considered [10]:

$$\begin{aligned} \frac{\mathrm{d}a}{\mathrm{d}t} &= \frac{2a^2 v}{\mu} a_t \\ \frac{\mathrm{d}e}{\mathrm{d}t} &= \frac{1}{v} 2(e + \cos f) a_t \\ \frac{\mathrm{d}\omega}{\mathrm{d}t} &= \frac{1}{ev} 2 \sin f \, a_t \\ \frac{\mathrm{d}E}{\mathrm{d}t} &= \frac{na}{r} - \frac{1}{ebv} 2a \sin f \, a_t \end{aligned} \tag{2}$$

where f is the true anomaly, ω is the argument of pericentre, $n = \sqrt{\mu/a^3}$ is the mean motion of the spacecraft, v is the magnitude of the orbital velocity, r is the orbital radius, and b is the semi-minor axis. The equations for inclination i and right ascension of the ascending node Ω are not given because these elements are not affected by tangential thrust.

Note that, by neglecting small terms in thrust acceleration in the differential equation for E and substituting the polar equation of the orbit in eccentric anomaly, the same approximate time law in Eq. (1) is recovered. Consequently, the approximate time law is neglecting first-order terms in the thrust acceleration, which are instead the leading ones for the orbital elements in the analytical and semi-analytical solutions. This supports the observation from [2] that the errors in the differential time law were of higher order than those from the analytical solution.

To address this limitation, in this work the time law from Eq. (2) is used instead. Performing the change of independent variable, terms on the small thrust

acceleration will now appear in the denominator of the equations of motion. Expanding in power series of a_t, the resulting system of ODEs is:

$$\begin{aligned}\frac{\mathrm{d}a}{\mathrm{d}E} &= a_t \frac{2a^3}{\mu}\sqrt{1-e^2\cos^2 E} + \mathcal{O}(a_t^2)\\ \frac{\mathrm{d}e}{\mathrm{d}E} &= a_t \frac{2a^2(1-e^2)}{\mu}\sqrt{\frac{1-e\cos E}{1+e\cos E}}\cos E + \mathcal{O}(a_t^2)\\ \frac{\mathrm{d}\omega}{\mathrm{d}E} &= a_t \frac{2a^2\sqrt{1-e^2}}{\mu e}\sqrt{\frac{1-e\cos E}{1+e\cos E}}\sin E + \mathcal{O}(a_t^2)\end{aligned} \quad (3)$$

which coincides up to first order terms with that obtained using the approximate time law in Eq. (1). The difference lies in the terms of order 2 and higher, coming from the series expansion of the inverse of the last of Eq. (2). On the other hand, the differential equation for the time law $t(E)$ takes the form:

$$\frac{\mathrm{d}t}{\mathrm{d}E} = \frac{r}{an} + a_t \frac{2r^2 \sin f}{aben^2 v} + \mathcal{O}(a_t^2) \quad (4)$$

Recalling the polar equation of the orbit in eccentric anomaly, $r = a(1 - e\cos E)$, this equation coincides with the inverse of Eq. (1) only on the zeroth order term, showing that the first-order solution in [2] was not complete. Consequently, the results for semi-major axis, eccentricity, and argument of pericentre in the analytical tangential thrust model from [2] are already valid up to first order terms in thrust acceleration, and only the time law needs to be corrected to include the missing terms. For this reason, hereafter the original time law neglecting the acceleration terms in Gauss planetary equations will be referred to as zeroth-order time law.

The solutions for semi-major axis and eccentricity are expressed as [2]:

$$\begin{aligned}a(E) &= a_{ref} + \varepsilon\, K_a\, E + \varepsilon\, a_{osc}(E)\\ e(E) &= e_{ref} + \varepsilon\, K_e\, E + \varepsilon\, e_{osc}(E)\end{aligned} \quad (5)$$

where the thrust parameter $\varepsilon = a_t/(\mu/a_{ref}^2)$ has been introduced, and the subindex 'ref' denotes a constant, reference value. The coefficients of the linear secular terms can be computed in terms of the complete elliptic integrals of the first and second kind F[·] and E[·] as follows:

$$\begin{aligned}K_a &= \frac{4a_{ref}\,\mathrm{E}\left[e_{ref}^2\right]}{\pi}\\ K_e &= \frac{4\left(1-e_{ref}^2\right)}{e_{ref}\pi}\left(\mathrm{E}\left[e_{ref}^2\right] - \mathrm{F}\left[e_{ref}^2\right]\right)\end{aligned} \quad (6)$$

The terms $a_{osc}(E)$ and $e_{osc}(E)$ represent an oscillatory contribution, expressed as a power series in small reference eccentricity e_{ref}. The full expressions are provided in [2], and reported in Appendix A for the reader's convenience. Note that that e_{osc} contains all the harmonics in eccentric anomaly up to the order of the expansion, while a_{osc} only includes the even ones.

To derive the analytical time law in [2], the solutions for semi-major axis and eccentricity, Eq. (5), are introduced into the inverse of the time law in Eq. (1). Then, a series expansion in eccentricity is performed, and the resulting terms are integrated one by one. Finally, the apse line correction, corresponding to the change in argument of pericentre, is added. For the first-order time law, instead, we introduce Eq. (5) into Eq. (4), performing the change from a_t to ε. It is straightforward to check that some terms in ε^2 will appear when we substitute the solutions for semi-major axis and eccentricity into the second term of the right-hand side of $\mathrm{d}t/\mathrm{d}E$. These second order terms should not be retained, as we have already neglected second order terms in the rest of the model. Therefore, we take the series expansion in small thrust parameter up to first order, which gives raise to two well-separated contributions. The first one corresponds to the solution already presented in [2] (without the apse line correction). The second one comes from introducing the reference values of the orbital elements into the term of the time law explicitly dependent on thrust. The secular and oscillatory components of a and e are already scaled by the thrust parameter, so their contribution would be of second order. This new contribution to the time law can be integrated analytically, leading to:

$$\Delta t^* n_{ref} = \left.\frac{C_1 - C_2}{e^2(e\,c_E - 1)\sqrt{-1 - \frac{2}{-1 + e\,c_E}}}\right|_{E_0}^{E} \quad (7)$$

with

$$\begin{aligned}C_1 &= (-4 + e\,c_E)(-1 + ec_E)(1 + ec_E)\\ C_2 &= 6\sqrt{1 - e^2 c_E^2}\,\operatorname{asin}\left[\frac{\sqrt{1 - ec_E}}{\sqrt{2}}\right]\end{aligned}$$

where $c_E = \cos E$

The accuracy improvement obtained from the new model is qualitatively assessed through several test cases. In the first one, the exact time law obtained from the numerical integration of the full Gauss planetary equations, Eq. (2), is used as reference value to determine the error of the zeroth-order approximate time law, Eq. (1), and the first-order one, Eq. (4). In both cases, the approximate time law is integrated together with the differential equations in eccentric anomaly for semi-

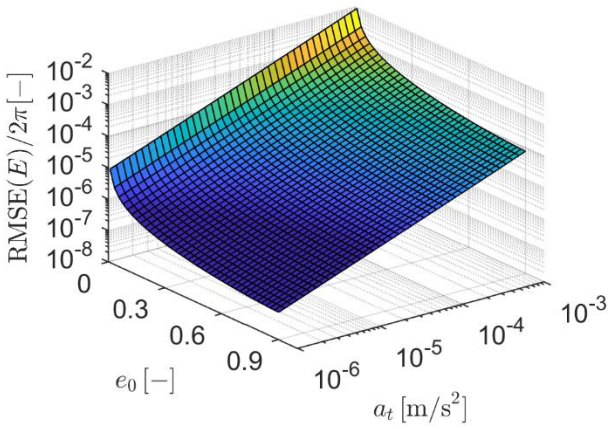

(a) Zeroth-order time law

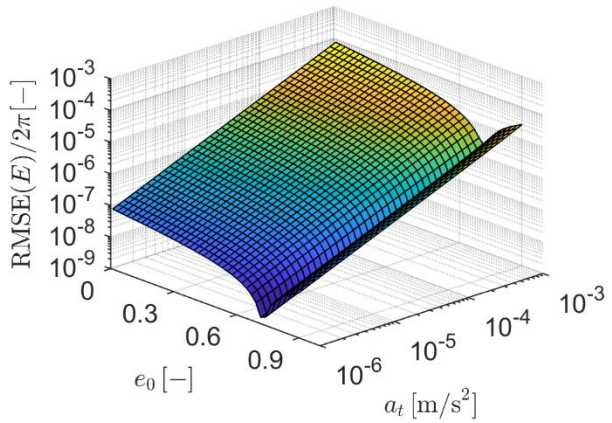

(b) Zeroth-order time law with apse line correction

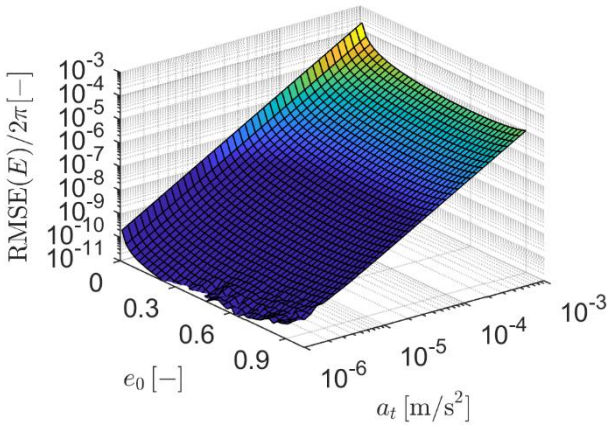

(c) First-order time law

Fig. 1. RMSE over 10 periods for the zeroth-order and first-order approximate differential time laws

major axis, eccentricity, and argument of pericentre, Eq. (3). The error is measured as the root-mean-square error (RMSE) between the exact and approximate time law over 10 orbital revolutions around Earth, with $\mu = 398{,}600.433\ \mathrm{km}^3/\mathrm{s}^2$, for an initial semi-major axis of 10,000 km and several values of thrust acceleration and initial eccentricity. The rest of initial orbital elements will not affect the time law under the force model used. It must be noted that a large range of initial eccentricities up to 0.9 is considered in order to assess the mathematical performance of the time laws, but many of these values will not correspond to physically valid orbits. Particularly, for the given value of initial semi-major axis, any orbit with an initial eccentricity higher than 0.34 would present an altitude at pericentre below 200 km.

The results in Fig. 1 show a clear improvement in accuracy as we move from the zeroth-order time law to the zeroth-order one with apse line correction, and finally to the first-order time law. Particularly, the apse line correction successfully reduces the significant error of the zeroth-order time law for quasi-circular and small eccentricity orbits. The physical reason is that the line of apses shows more mobility due to perturbations as the orbit becomes closer to the circular case, where the line of apses is not properly defined and Gauss planetary equations become singular. The zeroth-order time law with apse line correction also shows significant errors for eccentricities close to 1. However, this is not a practically relevant scenario for collision avoidance activities of Earth-bound objects, where the highest eccentricities we typically find are those of GTOs, with e around 0.73. Interestingly, the error surface shows a rift with global minima of the errors around these values of initial eccentricity.

The new first-order solution, instead, shows a more regular and smooth behaviour, no longer presenting the rift, and providing significantly smaller errors in general. The only exceptions are the regions $e \approx 0$ and $e \approx 0.73$ for high values of the thrust acceleration, where the zeroth-order time law with apse line correction outperforms the first-order one. This is particularly interesting for the quasi-circular case, because it shows that the mathematical formulation of the zeroth-order model with apse line correction is less affected by the circular orbit singularity in Gauss planetary equations. Indeed, the first-order time law displays a region of fast growth of the RMSE towards the lower end of the range, corresponding to $e_0 = 0.01$. This suggests the practical approach of using the zeroth-order time law with apse line correction for the case of quasi-circular orbits and high thrust acceleration, and the first-order one for the remainder of the range in e_0. Finally, it can be observed that the errors increase slightly towards the high-eccentricity end of the range, consistently with the behaviour of the zeroth-order model with apse line correction.

Table 1. Keplerian orbital elements of spacecraft and debris at CA

Object	a [km]	e [-]	i [deg]	Ω [deg]	ω [deg]	f_0 [deg]
Molniya 2-9	23236.962	0.66819	64.209	286.999	285.583	14.043
Debris	12962.638	0.31805	84.017	286.871	282.796	76.864

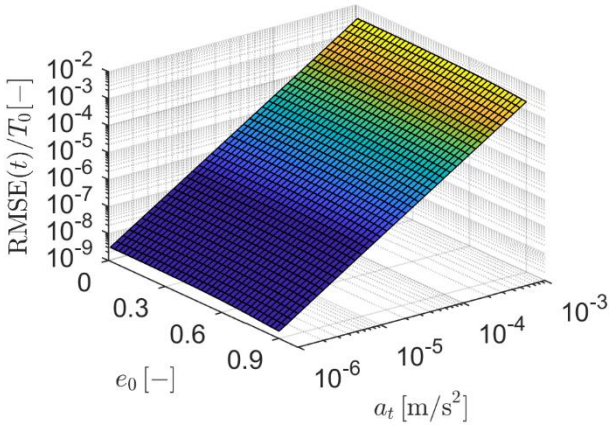

Fig. 2. RMSE over 10 periods of the first-order analytic time law

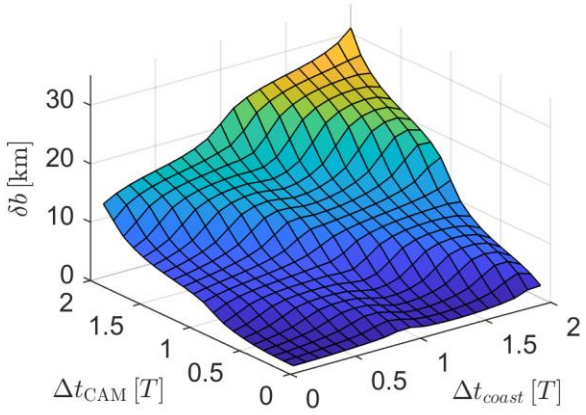

Fig. 3. Displacements in the encounter plane, for the nominal CA in Table 1 and $a_t = 10^{-6}$ m/s^2

The previous test served to evaluate the error incurred due to the use of an approximate time law for the change of independent variable in the equations of motion. Instead, the error of the analytical solution with respect to the exact numerical integration for the first-order time law is represented in Fig. 2. The results correspond to an expansion for $t(E)$ up to forth order in e_{ref}, which allows to reproduce up to the sixth harmonic in eccentric anomaly. It is observed that the error is higher than the one due to the introduction of the approximate differential time law, addressing the issue identified in [2]. In other words, the accuracy of the solution is now limited by the quality of the analytic approximation, and not the dynamical model. The error of the analytical solution could be reduced by increasing the order of the expansion in e_{ref}, but numerical tests reveal that the gains are small. Alternatively, the expansion could be avoided by using the full expressions in incomplete elliptic integrals of the first and second kind for a and e, as developed in [2]. However, this would have a penalty in computational cost because the time law would no longer reduce to an analytical expression and a numerical quadrature procedure would be required (i.e., semi-analytical model). Finally, the accuracy of both the differential time law and the analytical solution could be further improved by moving to a second-order model in thrust acceleration.

To close this section, the performance of the first-order and zeroth-order (with apse line correction) time laws is compared for a practical collision avoidance scenario. We consider a nominal zero-miss-distance CA taken from [2], between object "Molniya 2-9" (NORAD ID 7276) and a debris. The Keplerian elements for the spacecraft are retrieved from Space-Track [11] at epoch 2021-05-09, 17:32:21, while the debris has been generated setting a random relative velocity at CA. The resulting initial orbital elements of spacecraft and debris are reported in Table 1. Given this CA, the spacecraft performs a low-thrust CAM composed of a single thrusting arc of duration Δt_{CAM} and constant tangential acceleration magnitude a_t, followed by a coasting arc of duration Δt_{coast} up to the TCA. Fig. 3 depicts the achievable miss distances δb in the encounter plane (i.e., the plane perpendicular to the relative velocity of the spacecraft with respect to the debris at the nominal CA), for a fixed thrust acceleration of 10^{-6} m/s^2, and different durations of the coast arc and thrust arc. These results are computed using the new model with the first-order time law. As expected, the achievable deviation grows both with Δt_{CAM}, which implies a higher consumption of propellant, and Δt_{coast}. Furthermore, the solution shows some characteristic oscillatory patterns, due to the different effect of thrusting close to the pericentre or the apocentre.

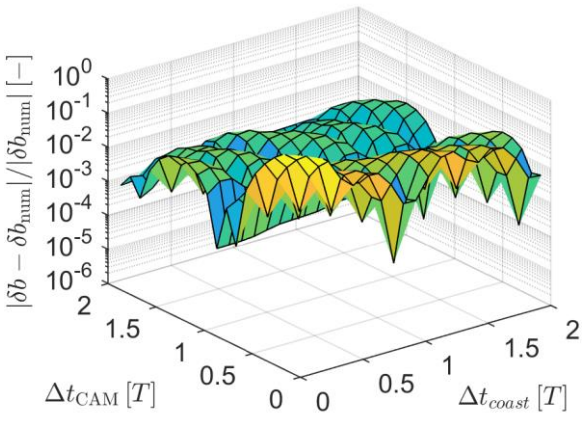

(a) Zeroth-order time law with apse line correction

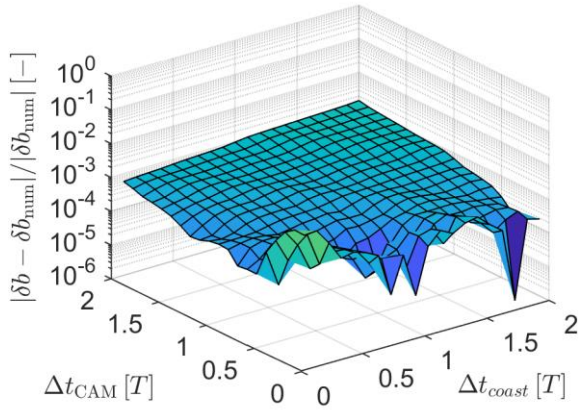

(b) First-order time law

Fig. 4. Relative errors of the displacement in the encounter plane for the zeroth-order (with apse line correction) and first-order time laws, for the nominal CA in Table 1 and $a_t = 10^{-6}$ m/s^2

The accuracy of both analytical models is quantified in Fig. 4, in terms of the relative error in the predicted displacement compared to a high-accuracy numerical evaluation. As expected, the first-order time law presents relative errors significantly smaller than those of the zeroth-order model with apse line correction. Interestingly, the errors of both models are highest for very short thrust and coast arc times; in these cases, the conceptual validity of the averaging procedure is limited.

2.2 A first exploration of normal-thrust CAMs

Once the first-order model for tangential thrust is completed in a consistent way, the next step would be to include the effects of thrust actions in directions other than tangential. Still considering a manoeuvrer without change of plane, an analytical model for a normal thrust action is sought for. The normal direction is defined as:

$$\hat{\mathbf{n}} = \frac{\mathbf{h}}{h} \times \frac{\mathbf{v}}{v} \tag{8}$$

where $\mathbf{h}$ and h are the angular momentum vector and magnitude, respectively. For a first-order approximation in the total magnitude of the thrust acceleration, the contributions in a_t and a_n become decoupled, and the single-averaged analytical solutions for tangential and normal thrust can be computed separately. The non-zero Gauss planetary equations for a normal thrust action take the form [10]:

$$\begin{aligned} \frac{\mathrm{d}e}{\mathrm{d}t} &= -a_n \frac{r \sin f}{av} \\ \frac{\mathrm{d}\omega}{\mathrm{d}t} &= a_n \frac{\left(2e + \frac{r}{a}\cos f\right)}{ev} \\ \frac{\mathrm{d}E}{\mathrm{d}t} &= \frac{an}{r} - a_n \frac{r(e + \cos f)}{bev} \end{aligned} \tag{9}$$

Same as before, to perform the change of independent variable to eccentric anomaly we take the inverse of the differential equation for E and expand it in power series of the thrust acceleration up to first order terms, yielding:

$$\frac{\mathrm{d}t}{\mathrm{d}E} = \frac{r}{an} + \frac{r^3(e + \cos f)}{a^2 ben^2 v} + \mathcal{O}(a_n^2) \tag{10}$$

As expected, the zeroth-order term coincides with that of the tangential case, Eq. (4). Introducing this relation for the change of independent variable and retaining terms up to order one in a_n, the differential equations for eccentricity and argument of pericentre take the form:

$$\begin{aligned} \frac{\mathrm{d}e}{\mathrm{d}E} &= a_n \frac{a^2(-1 + e\,c_E)\,s_E}{\mu\sqrt{\frac{1 + e\,c_E}{(-1 + e^2)(-1 + e\,c_E)}}} + \mathcal{O}(a_n^2) \\ \frac{\mathrm{d}\omega}{\mathrm{d}E} &= -a_n \frac{a^2(e + c_E)(-1 + e\,c_E)}{e\,\mu\sqrt{-1 - \frac{2}{-1 + e\,c_E}}} + \mathcal{O}(a_n^2) \end{aligned} \tag{11}$$

where $s_E = \sin E$. It is straightforward to solve the first equation analytically using a symbolical manipulator, reaching:

$$e(E) = \varepsilon_n \frac{C_1 + C_2}{2e(-1 + ec_E)\sqrt{\frac{1 + e\,c_E}{(-1 + e^2)(-1 + e\,c_E)}}} \tag{12}$$

where C_1 and C_2 coincide with those defined in Eq. (7), and $\varepsilon_n = a_n/(\mu/a_{ref}^2)$ is a non-dimensional thrust parameter.

Analytic solutions can also be achieved for the argument of pericentre and the time law $t(E)$. However, they have long and cumbersome expressions, involving incomplete elliptic integrals of the first and second kind, as well as inverse trigonometric functions. For brevity, they are not reproduced here. While they are valid solutions, their functional form defeats the purpose of building a highly efficient model. Future works will focus on the approximate decomposition of these expressions, aiming to reach simpler expressions similar to those for the tangential case.

3. On-board applications. The e.Cube mission

The analytical model for low-thrust tangential CAM can be suitable for on-board implementation given its simple algorithmic structure and reduced computational cost. However, total on-board CAM autonomy is not limited to the design and optimization of the manoeuvre, but also requires the capability to autonomously decide if and when said CAM is required. Recent works by different authors have studied the possibility of performing this task using artificial intelligence (AI) and machine learning (ML) techniques [12], taking as input data a series of Conjunction Data Messages (CDMs). Although some promising results have been obtained, two key issues remain: the selection of the most appropriate AI/ML algorithm, and the lack of real-world data to train it.

A framework for autonomous on-board collision avoidance operations is proposed based on two modules: a ML-powered decision-making module, and a CAM design module. Testing this framework is one of the goals of the e.Cube mission, a CubeSat demonstration mission recently proposed by the COMPASS group in collaboration with several Italian partners [13]. The goal of e.Cube is to contribute to the advancement of technologies and methodologies dedicated to space debris mitigation and remediation, through three experiments: 1) on-board autonomous collision avoidance capabilities; 2) untraceable space debris in-situ detection, acquiring data to support current and future models for small debris; 3) re-entry characterization, providing direct measurements on the atmospheric conditions and the spacecraft mechanical behaviour.

The collision avoidance experiment consists of several in-flight impulsive CAM tests for simulated CAs with a virtual debris. The CA is characterized by a sequence of CDM-like messages, uploaded to e.Cube from ground. Based on them, the decision-making module determines if the predicted risk at TCA may become unacceptable, triggering the design and execution of a CAM. The CAM design module leverages the same framework used in this work [1], but formulating the dynamics with the impulsive CAM analytical models in [4]. Although low-thrust CAMs will not be tested, the results will serve to validate both the CAM design framework and the decision-making module, as well as the interaction between them.

4. Conclusions

A fully analytical model for low-thrust CAMs under a tangential thrust orientation control law has been presented. It is based on Gauss planetary equations, expressed in terms of the eccentric anomaly and single-averaged over one revolution. This model is the last iteration in a series of analytical and semi-analytical formulations, being the key novelty that the differential time law, needed to change the independent variable from time to eccentric anomaly before averaging, includes up to first order terms in the thrust acceleration. Previous models used a differential time law that neglected the direct contribution of thrust, and relied on a correction of the apse line position through the variation of the argument of periapsis to account for these effects. Numerical tests show that the first-order time law provides in general significant improvements with respect to the previous, zeroth-order time law, particularly for small thrust acceleration. The one significant exception is quasi-circular orbits, for which the zeroth-order time law with apse line correction is less affected by the numerical issues linked to the singularity of Gauss equations for circular orbit. This suggests the use of the zeroth-order time law for very-low-eccentricity scenarios, and the first-order one for the rest. These findings are sustained by different numerical test scenarios.

Once the tangential thrust case is fully characterized, the next step is to include normal components in the thrust acceleration. Although low-thrust CAMs are usually aligned close to the tangential direction, an optimal solution will also contain small components in the other directions. Analytical solutions for the Keplerian elements affected by a normal thrust acceleration have been obtained; however, their expressions are too cumbersome to be used for a highly efficient computational implementation. Further work is needed to reduce these exact, analytical solutions into approximate ones that are suitable for manipulation and efficient CAM computation and design.

The simple implementation and high computational efficiency of the tangential low-thrust CAM model make it suitable for on-board applications. A framework for autonomous on-board collision capabilities, part of the e.Cube CubeSat demonstration mission, has been presented. This framework is composed of a ML-powered decision-making module, and a CAM design module based on analytical models.

Acknowledgements

This project has received funding from the European Research Council (ERC) under the European Union's Horizon 2020 research and innovation programme (grant agreement No 679086 – COMPASS).

Appendix A

This appendix presents a summary of the expressions for the tangential low-thrust CAM analytical model. For a detailed derivation of these expressions and additional details, the reader can refer to [2].

The general expressions for semi-major axis and eccentricity were already presented in Eq. (5), while the slopes K_a and K_e of the mean, linear evolution correspond to Eq. (6).The oscillatory components are of the form:

$$\begin{aligned} a_{osc}(E) &= \sum_{u=1,2,..} e_{ref}^{2u} \sum_{w=1}^{u} K_{uw}^{a} \sin 2wE \\ e_{osc}(E) &= \sum_{u=1,2,..} e_{ref}^{u-1} \sum_{w=1}^{u} K_{uw}^{e} \sin wE \end{aligned} \tag{13}$$

with coefficient matrices up to order 6 (the coefficients up to order 8 can be found in [2]):

$$K^a = a_{ref} \begin{bmatrix} -\frac{1}{4} & 0 & 0 \\ -\frac{1}{16} & -\frac{1}{128} & 0 \\ -\frac{15}{512} & -\frac{3}{512} & -\frac{1}{1536} \end{bmatrix}$$

$$K^e = \begin{bmatrix} 2 & 0 & 0 & 0 & 0 & 0 \\ 0 & -\frac{1}{2} & 0 & 0 & 0 & 0 \\ -\frac{5}{4} & 0 & \frac{1}{12} & 0 & 0 & 0 \\ 0 & \frac{1}{4} & 0 & -\frac{1}{32} & 0 & 0 \\ -\frac{9}{32} & 0 & -\frac{1}{192} & 0 & \frac{3}{320} & 0 \\ 0 & \frac{19}{256} & 0 & -\frac{1}{256} & 0 & -\frac{1}{256} \\ -\frac{65}{512} & 0 & -\frac{5}{512} & 0 & \frac{11}{2560} & 0 \end{bmatrix}$$

Note that the values a_{ref} and e_{ref} can be obtained imposing the initial conditions $a(E_0; a_{ref}, e_{ref}) = a_0$ and $e(E_0; a_{ref}, e_{ref}) = e_{ref}$.

The expression for the argument of pericentre takes the form:

$$\Delta\omega = \varepsilon \frac{2\sqrt{1-e_{ref}^2}}{e_{ref}^2} \left(2 \operatorname{asin} \sqrt{\frac{1-e_{ref}c_E}{2}} - \sqrt{1-e_{ref}^2 c_E^2} \right) \Bigg|_{E_0}^{E} \tag{14}$$

Finally, the expression for the zeroth-order time law (without the apse line correction) is:

$$\begin{aligned} \Delta t\, n_{ref} &= E - e_{ref} \sin E + \\ &+ \varepsilon \left[E^2 \frac{3}{4} \frac{K_a}{a_{ref}} - E \left(K_e + \frac{3}{2} e_{ref} \frac{K_a}{a_{ref}} \right) \sin E \right. \\ &\left. + \sum_{u=1,..} e_{ref}^{u-1} \sum_{w=1}^{u} K_{uv}^{E} \cos wE \right] \Bigg|_{E_0}^{E} \end{aligned} \tag{15}$$

with coefficients up to third order in e_{ref} (the coefficients up to order 4 can be found in [2])

$$K^E = \begin{bmatrix} -K_e & \frac{1}{2} & 0 & 0 & 0 \\ -\frac{3+\frac{18K_a}{a_{ref}}}{12} & 0 & 1/12 & 0 & 0 \\ 0 & -\frac{5}{48} & 0 & \frac{1}{96} & 0 \\ -1/16 & 0 & -\frac{5}{192} & 0 & -\frac{1}{320} \end{bmatrix}$$

References

[1] J.L. Gonzalo, C. Colombo, and P. Di Lizia, Introducing MISS, a new tool for collision avoidance analysis and design, Journal of Space Safety Engineering, 7, 3 (2020) 282–289. https://doi.org/10.1016/j.jsse.2020.07.010

[2] J.L. Gonzalo, and C. Colombo, Lightweight algorithms for collision avoidance applications, 11th ESA GNC, virtual conference, 2021, 22-25 June.

[3] J. L. Junkins, and H. Schaub, Analytical mechanics of space systems. American Institute of Aeronautics and Astronautics, Reston, VA, 2009.

[4] J.L. Gonzalo, C. Colombo, and P. Di Lizia, Analytical framework for space debris collision avoidance maneuver design, Journal of Guidance, Control and Dynamics, 44, 3 (2021) 469-487. https://doi.org/10.2514/1.G005398

[5] J.L. Gonzalo, C. Colombo, and P. Di Lizia, Analysis and design of collision avoidance manoeuvres for passive de-orbiting missions, Astrodynamics 2018, series Advances in the Astronautical Sciences, 167 (2019) 2189-2208. AAS/AIAA Astrodynamics Specialist Conference, Snowbird, UT, 2018, 18–23 August.

[6] J.L. Gonzalo, C. Colombo, and P. Di Lizia, A semi-analytical approach to low-thrust collision avoidance manoeuvre design, 70th International Astronautical Congress, Washington, D.C., USA, 2009, 21–25 October. Paper number IAC-19-A6.2.3

[7] S. Huang, C. Colombo, and F. Bernelli-Zazzera, Orbit raising and de-orbit for coplanar satellite constellations with low-thrust propulsion, IAA-AAS-DyCoSS4-1-15, 4th IAA Conference on Dynamics and Control of Space Systems, Changsha, China, 2018, 21–23 May.

[8] S. Huang, C. Colombo, E.M. Alessi, and Z. Hou, Large constellation de-orbiting with low-thrust propulsion, AAS 19-480, 29th AAS/AIAA Space Flight Mechanics Meeting, Ka'anapali, HI, 2019, 13–17 January.

[9] C. Colombo, M. Vasile, and G. Radice, Semi-analytical solution for the optimal low-thrust deflection of near-Earth objects, Journal of Guidance, Control and Dynamics, 32, 3 (2009) 796-809. https://doi.org/10.2514/1.40363

[10] R. H. Battin, An introduction to the mathematics and methods of Astrodynamics, AIAA Education series, AIAA, Reston, VA, 1999.

[11] Space-Track, https://www.space-track.org, (accessed 09.05.21)

[12] T. Uriot, et al., Spacecraft collision avoidance challenge: Design and results of a machine learning competition, Astrodynamics, 2021. https://doi.org/10.1007/s42064-021-0101-5

[13] C. Colombo, et al., e.Cube mission: the Environmental CubeSat, 8th ECSD, ESA/ESOC, Darmstadt, Germany 2021, 20-23 April.